



Original Article

Promotion of hMDSC differentiation by combined action of scaffold material and TGF- β superfamily growth factorsAirina Mazetyte-Godiene ^{a, b, c, *}, Agne Vailionyte ^b, Tadas Jelinskas ^c, Jaroslav Denkovskij ^d, Arvydas Usas ^a^a Institute of Physiology and Pharmacology, Medical Academy, Lithuanian University of Health Sciences, Kaunas, Lithuania^b UAB Ferentis, Savanoriu ave. 235, Vilnius, Lithuania^c Department of Nanoengineering, Center for Physical Sciences and Technology, Vilnius, Lithuania^d Department of Regenerative Medicine, Centre for Innovative Medicine, Vilnius, Lithuania

ARTICLE INFO

Article history:

Received 3 August 2023

Received in revised form

8 January 2024

Accepted 17 March 2024

ABSTRACT

Objective: Herein we propose a combined action of collagen type I (CA) or synthetic collagen-like-peptide functionalized with the cell adhesive RGD motif (PEG-CLP-RGD) hydrogels and selected growth factors to promote chondrogenic differentiation of human muscle-derived stem cells (hMDSCs) under normal and reduced oxygen conditions.

Methods: hMDSCs were set for differentiation towards chondrogenic lineage using BMP-7 and TGF- β 3. Cells were seeded onto hydrogels loaded with growth factors (75ng/scaffold) and cultured for 28 days under normal (21%) and severe hypoxic (1%) conditions. Chondrogenesis was evaluated by monitoring collagen type II and GAG deposition, and quantification of ACAN expression by RT-PCR.

Results: Sustained release of TGF β 3 from the hydrogels was observed, $8.7 \pm 0.5\%$ of the initially loaded amount diffused out after 24 h from both substrates. For the BMP-7 growth factor, $14.8 \pm 0.3\%$ and $18.2 \pm 0.6\%$ of the initially loaded amount diffused out after 24 h from CA and CLP-RGD, respectively. The key findings of this study are: i) the self-supporting hydrogels themselves can stimulate hMDSC chondrogenesis by inducing gene expression of cartilage-specific proteoglycan aggrecan and ECM production; ii) the effect of dual BMP-7 and TGF- β 3 loading was more pronounced on CA hydrogel under normal oxygen conditions; iii) dual loading on PEG-CLP-RGD hydrogels did not have the synergistic effect, TGF- β 3 was more effective under both oxygen conditions; iv) BMP-7 can improve chondrogenic effect of TGF- β 3 on CA scaffolds, and hydrogels loaded with both growth factors can induce cartilage formation in hMDSC cultures.

Conclusion: Our results support the potential strategy of combining implantable hydrogels functionalized with differentiation factors toward improving cartilaginous repair.

© 2024, The Japanese Society for Regenerative Medicine. Production and hosting by Elsevier B.V. This is an open access article under the CC BY-NC-ND license (<http://creativecommons.org/licenses/by-nc-nd/4.0/>).

1. Introduction

Cartilage is a non-vascular highly-organized tissue composed of specialized cells - chondrocytes. The low cellularity and lack of blood vessels, lymphatic vessels, and nerves result in limited cartilage self-regeneration. Age, damage from trauma or degenerative diseases lead to joint pain, functional impairment, and

osteoarthritis; due to aging world population these issues affect an increasing number of people [1]. Although different options are available to treat cartilage lesions (microfracture chondroplasty, mosaicplasty, matrix-assisted autologous chondrocyte transplantation, miscellaneous scaffold-based techniques [2–4]), no current method can fully restore the anatomical structure and mechanical function of the native hyaline cartilage. Therefore, there is a need for new approaches, such as employing advanced biomaterials containing bioactive cues, e.g., growth factors (GFs) or other bioactive molecules, to guide cartilage formation [5].

Growth factors are biologically active polypeptides produced by the body that can stimulate cellular division, growth, and

* Corresponding author.

E-mail address: airina.mazetyte@lsmu.lt (A. Mazetyte-Godiene).

Peer review under responsibility of the Japanese Society for Regenerative Medicine.

differentiation [6]. They include the transforming growth factor-beta family (TGF- β), insulin-like growth factor-1 (IGF-1), fibroblast growth factor (FGF), platelet derived growth factor (PDGF), bone morphogenic protein-2 (BMP-2), bone morphogenic factor-7 (BMP-7), which play fundamental roles in cartilage and chondrocytes biology [4,7,8]. The use of TGF- β growth factor for cartilage regeneration has been extensively investigated and multiple studies have demonstrated that TGF- β promotes cartilage formation *in vitro* and *in vivo* [7,9–11]. BMPs are known for their ability to induce ectopic bone and cartilage formation; BMP-2 and BMP-7 induce osteogenic/chondrogenic differentiation and bone/cartilage formation, although they demonstrate preferential affinity for different receptors [12]. There are several methods for the delivery of growth factors: freeform medium, physical blending in a hydrogel, covalent bonding to a hydrogel, etc [8]. Covalent bonding helps to avoid quick diffusion and allows operating at low doses of GF, while still promoting cell proliferation and extracellular matrix (ECM) production. Meanwhile, GF delivery by encapsulating in hydrogels leads to sustained release for up to several months but will get significantly reduced with time. However, regeneration of complex tissues may require delivery of multiple GFs using different strategies [13].

Soft bioactive materials emerged over the past years as a possible solution for regeneration of articular cartilage. For example, various forms of collagen-based materials have been available for cartilage defect repair, including sponges, membranes, hydrogels, etc [14]. Articular cartilage is mainly composed of collagen type II, which displays better chondrogenicity than collagen type I. Nevertheless, both of these collagen types can maintain chondrocyte phenotypes and support chondrogenic differentiation of human mesenchymal stem cells [15,16]. Bioactive sites in the collagen triple helix structure affect cell behavior. Short peptides such as RGD (Arg-Gly-Asp, fibronectin-binding domain) and DGEA (Asp-Gly-Glu-Ala) can also support cell attachment and growth. Kudva et al. demonstrated that RGD-functionalized PEG hydrogels can enhance cell proliferation, glycosaminoglycan synthesis and chondrogenic gene expression [17]. Moreover, a recent study suggests that fibronectin 1 plays a significant role in cartilage regeneration through its activation via integrins $\alpha 5\beta 1$ and $\alpha V\beta 3$ [18].

In this study, we have focused on the applicability of chemically crosslinked hydrogels as a self-supporting carrier matrix for stem cell differentiation. In our experiments we used skeletal muscle-derived stem cells (MDSCs) - mesenchymal stem cell lineage [19]. Previous studies explored chondrogenic differentiation potential of human and rabbit MDSCs and showed that these cells can differentiate into the cartilage-like tissue *in vitro* and *in vivo* [9,20].

Chondrocytes *in vivo* reside in a hypoxic environment (1–10% O_2), thus, it has been suggested that exposing stem cells to hypoxia may also contribute a beneficial effect on their differentiation. Hypoxia-inducible factor-1 α (HIF-1 α) has a key role in both differentiation of progenitor cells and maintaining a chondrogenic phenotype once differentiated [21]. Moreover, hypoxia may affect chondrocyte maturation and function [22].

Based on the above literature data, we chose to explore the chondrogenic capacity of hMDSCs on the hydrogel constructs under normal oxygen vs. hypoxia conditions. We cultivated these cells on hydrogels consisting of either collagen type I (CA) or of synthetic peptides that have the collagen-like peptide (CLP) sequence. The latter non-specific binding sequence was further functionalized with cell adhesive RGD motif (PEG-CLP-RGD). We compared the effects on hMDSC differentiation by combining the different hydrogels with TGF- $\beta 3$ or/and BMP-7 growth factors (Fig. 1). Previously, TGF- $\beta 3$ and BMP-7 were used in a dual study by Crecente-Campo and results showed efficient cartilage formation in human mesenchymal stem cell cultures [13].

2. Materials and methods

2.1. PEG-CLP, PEG-CLP-RGD and CA synthesis

Peptide synthesis, conjugation to PEG, synthesis of PEG-CLP and PEG-CLP-RGD hydrogels, and the characterization were performed following the protocols that were previously described [23–26]. CLP (Cys-Gly-(Pro-Lys-Gly)₄(Pro-Hyp-Gly)₄(Asp-Hyp-Gly)₄ and CLP-RGD peptides (Cys-Gly-(Pro-Lys-Gly)₄(Pro-Hyp-Gly)₄(Asp-Hyp-Gly)₄-Arg-Gly-Asp-Ser-Pro-Gly) were synthesized by UAB Ferentis (Vilnius, Lithuania).

Collagen I-based hydrogels of 8.5% (w/w) (CA) were produced following the published protocol [27] using 4-(4,6-dimethoxy-1,3,5-triazin-2-yl)-4-methylmorpholinium chloride (DMTMM) (Merck KGaA) as the crosslinking agent.

After PEG-CLP-RGD, PEG-CLP and CA crosslinking, 6 mm hydrogel disks were cut from the fabricated sheets using a surgical trephine. Prior to use, hydrogels were kept refrigerated inside sterile vials with phosphate buffer solution (PBS, pH 7.4) containing 1% (v/v) chloroform to maintain sterility.

2.2. Insertion and release of BMP-7 and TGF- $\beta 3$ growth factors

Different strategies were tested to embed the growth factors in the CA and PEG-CLP-RGD hydrogels. In the first group, the hydrogels were prepared as described above and 150 ng/mL of BMP-7 (Gibco) or TGF- $\beta 3$ (Abcam) were mixed into the hydrogel solution before casting (mixed-in group). In the second group, the prepared hydrogel disks were resuspended in a solution of “growth factor” buffer (500 μ L of sterile-filtered PBS (pH 7.4) supplemented with 150 ng/mL BMP-7 or TGF- $\beta 3$ and 0.1% bovine serum albumin (BSA)). The caps were wrapped in parafilm to avoid evaporation and the tubes were placed in a cell culture incubator (37 °C) for 24 h (solution group). In the third group, different concentrations of the growth factors (150, 100 and 75 ng/mL) were placed onto dried hydrogels and left for 2 h in the cell culture incubator (37 °C) to slowly sink in (sink-in group). After growth factor insertion, the samples were transferred into a fresh 24-well plate and the wells were filled with hMDSCs growth medium. At designated time points, the medium was collected and replaced with fresh medium, storing the collected medium at –80 °C until further analysis. Following the collection of all samples, they were thawed and the release of TGF- $\beta 3$ and BMP-7 was measured in the medium (samples were diluted with fresh hMDSCs medium to achieve a concentration of 6000 pg/mL for BMP-7 and 2000 pg/mL for TGF- $\beta 3$, which are the maximum of the standard curves) using an Enzyme Linked Immunosorbent Assays (Thermo Scientific and OmniKine, respectively) following manufacturer's protocols.

The amount of GFs remaining inside the hydrogels was assessed after digestion using 0.2% collagenase XI (Merck) solution in Hanks' balanced salt solution (HBSS (Gibco)) 2 h at 37 °C. After digestion, the supernatant was collected, wells were washed with PBS buffer (which was also collected), and centrifugated at 1000 g for 15 min. The supernatants were frozen at –80 °C until analysis using ELISA.

2.3. *In vitro* cell studies

2.3.1. hMDSC isolation and expansion

Adult human skeletal muscle tissue samples were obtained during anterior cruciate ligament reconstruction procedure performed on a 53-year-old male, after informed consent for the biopsy material to be used in laboratory research. The ethical consent was approved by the Regional Medical Ethics Committee (No. BE-2-22). The samples were processed within a few hours after surgery and hMDSCs were isolated by strictly following the previously

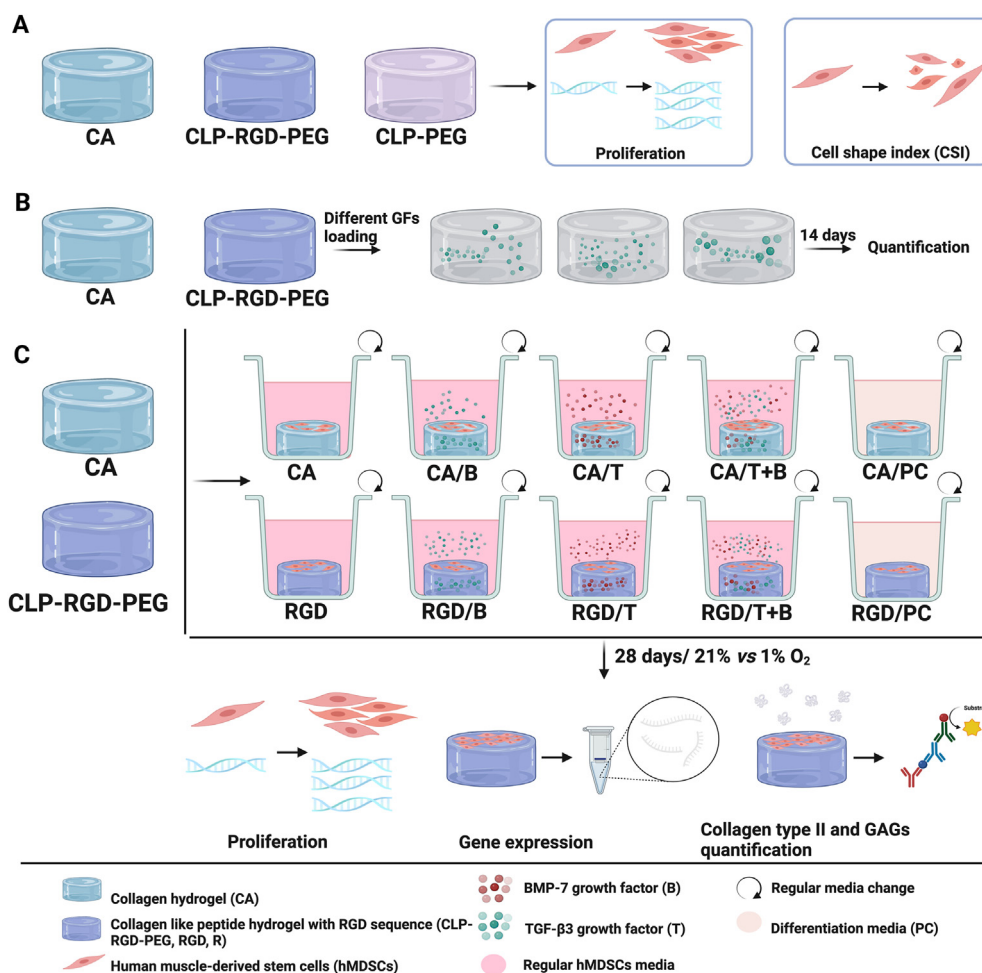


Fig. 1. Schematic explaining the design of the study. (A) Human muscle derived-stem cells (hMDSCs) were seeded on CA, PEG-CLP, and PEG-CLP-RGD hydrogels for cell proliferation and cell shape index (CSI) experiments; (B) Acellular constructs were used for characterization of BMP-7 and TGF-β3 growth factor release; (C) The hMDSCs were seeded on CA and PEG-CLP-RGD hydrogels containing growth factors and incubated for 28 days under normal oxygen or hypoxia conditions. Chondrogenesis was evaluated by characterizing matrix deposition using biochemical assays and measuring chondrogenic gene expression using RT-qPCR. Created with BioRender.com.

reported pre-plate technique [28]. In the last cell fraction, the cells that were slowest to adhere to the collagen-coated flasks, i.e. pre-plate 6 (pp6), were expanded up to 6–10 passages and used for further differentiation experiments. The cells were cultivated in a monolayer on a collagen-coated surface using Dulbecco's modified Eagle's medium (DMEM) with 4.5 g glucose/L (Gibco), supplemented with 10% fetal bovine serum (FBS) (Gibco), 10% horse serum (HS) (ThermoFisher Scientific), 0.5% chicken embryo extract (CEE) (Life Science Production), and 1% penicillin/streptomycin (P/S (10,000 U/L) (Gibco)) at 37°C, 5% CO₂, in a humidified Binder C150 incubator, changing the culture medium every 2–3 days.

For visualization and live cell staining, the cells on hydrogels were incubated with Calcein AM reagent (Invitrogen). Dye was diluted to a final 5 μM working concentration with serum free DMEM and incubated with cells for 90 min. Images were recorded using an Olympus BX 51 upright microscope.

2.3.2. Seeding and chondrogenic differentiation of hMDSCs on the CA and PEG-CLP-RGD hydrogels

In order to characterize the isolated cell phenotypes, CD34 (ThermoFisher Scientific), CD45 (ThermoFisher Scientific), CD59 (Bioscience), CD90 (Abcam) and CD117 (ThermoFisher Scientific) cell surface markers were analysed. After counting, the cells were resuspended in 2 mL of 1% of BSA in PBS and stained with the

commercially available fluorochrome-labelled antibodies or corresponding isotype controls for 30 min at 4°C in the dark. After incubation, the cells were washed twice with 1% BSA in PBS and stained with 7-aminoactinomycin D (7-AAD (BD Pharmingen)) for 20 min to exclude any dead cells. After incubation with 7-AAD, the cells were resuspended in 400 μL of 1% of BSA in PBS and analysed using FACS Aria III flow cytometer (BD Live Sciences, San Jose, USA) according to the manufacturer's instructions. The dead cells and debris were excluded using standard gating procedures. To make histograms 10,000 gated events were used. Data for isotype control sample were acquired to establish a reference for non-specific binding (2% positive rate point for isotype control). BD FACSDiva (BD Biosciences, USA) and FlowJo (Treestar, USA) software packages were employed for data analysis.

For *in vitro* studies, CA and PEG-CLP-RGD hydrogels, 6 mm in diameter and 500 μm in height, loaded with BMP-7 and TGF-β3 growth factors (75 ng/scaffold of each) were used. The number of cell-seeded constructs used for the characterization techniques is specified below. Before cell seeding, all hydrogels were washed in PBS buffer 3 times for 1 h. After washing, the hydrogels were transferred to a 48-well culture plate (TPP) and the growth factors were inserted. The cells were seeded on hydrogels at a density of 8×10^3 per scaffold. The constructs were kept in a cell culture incubator for 40 min and then the wells were filled with 1 mL of

hMDSC culture medium. The positive control scaffolds were cultured in chondrogenic differentiation medium (Gibco). No additional growth factors were added in the hMDSC culture medium during the experiments. The experiments were carried out under two different oxygen supply conditions: normal oxygen (21%, normoxia) and reduced oxygen (1%, hypoxia). After 1 week, the hypoxia group constructs were transferred into the cell culture incubator with 1% oxygen inside (Binder).

2.3.3. CCK8 and cell shape index (CSI) assays

CCK8 assay was performed on the cells on CA and PEG-CLP-RGD constructs. Before each time point, the constructs were transferred to a new 48-well plate and solution of 10% (v/v) CCK8 (Abcam), prepared in basal cell culture medium or chondrogenic differentiation medium, was transferred to the culture plates (300 μ L/scaffold). After 4 h of reaction with the cells at 37°C in the cell culture incubator, 100 μ L of CCK8 solution was taken from each well and placed in a 96-well plate (TPP) in duplicate. Absorption was measured in a microplate reader (Epoch, Biotek) at 460 nm. Cell culture medium was used as negative control.

The cell shape index was calculated by applying the equation:

$$\text{Shape index} = 4\pi A / P^2$$

where A is the cell area and P is the cell perimeter. The cell perimeter and area were calculated using ImageJ software. Cells were labeled with cell-permeant dye Calcein, AM (Invitrogen).

2.3.4. DMMB and ELISA assays

The amount of glycosaminoglycans (GAGs) deposited by the cells into the hydrogels was assessed using dimethylmethylene blue (DMMB) solution, prepared as previously described elsewhere [29]. The hydrogels were digested for 48 h at 60°C in 1 mL papain digestion solution, prepared by adding to each 50 mL of digestion buffer (200 mM of sodium phosphate monobasic buffer with 1 mM ethylenediaminetetraacetic acid (EDTA) (pH 6.8)), 50 mg papain (Sigma) and 48 mg of *n*-acetyl-cysteine (Sigma). After digestion, the samples were centrifuged at 6000 g for 10 min. Next, 60 μ L of each supernatant was transferred into a 96-well plate and 200 μ L of DMMB solution was added to each well. The absorbance at 595 nm was measured on the microplate reader (Epoch, Biotek) and the corresponding amount extrapolated from linear regression of the standard curve. The standard curve was prepared with chondroitin 4-sulphate (0–10 μ g/mL). The GAG contents were normalized to the DNA content detected on day 28.

The amount of type II collagen secreted by the cells into the cell culture medium was assessed using the Enzyme Linked Immunosorbent Assay (FineTest) according to the manufacturer's protocol. After thawing, the cell culture medium supernatant was centrifuged for 20 min at 1000 g at 4°C. Each sample was assessed in duplicate. The total amount of the type II collagen (deposited in 28 days) was normalized to the DNA content detected on day 28.

2.3.5. Gene expression with RT-PCR

The expression of mRNA for the genes of interest in the cells cultivated on the CA and PEG-CLP-RGD hydrogels was measured by real-time PCR analysis. After 28 days of culture, the scaffolds were washed with 1 \times PBS buffer. Total RNA was extracted from the cells using RNAqueous Micro Kit (Invitrogen) according to the manufacturer's protocol. The RNA concentration was quantified with a spectrophotometer (NanoDrop ND-1000, Thermo Scientific) and only samples with absorbance ratio 260:280 values between 1.9 and 2.1 were used for first-strand complementary DNA (cDNA) synthesis according to the protocol from the Maxima H minus First

strand cDNA synthesis kit (ThermoFisher Scientific) in a Prime Elite PCR system (Techne). Briefly, 300 ng of total RNA were reverse transcribed in a 20 μ L reaction volume. Afterwards, the obtained cDNA was used as a template for amplification of target genes using a Maxima SYBR green/ROX qPCR master mix (2 \times) with 0.3 μ M of both forward and reverse primers. The primers were sequence specific to each gene, namely, glyceraldehyde-3-phosphate (GAPDH, forward: ATGGGAAGGTGAAGGTCG; reverse: TAAAAG-CAGCCCTGGTGACC), COL1A1 (Col I, forward: CAGCCGCTCACCTA-CAGC; reverse: TTTTGTATTCAATCACTGTCTTGCC), ACAN (aggrecan, forward: TCGAGGACAGCGAGGCC; reverse: TCGAGGGTGTAGCGTGTAGAGA), VCAN (versican, forward: TGGAATGATGTTCCCTGCAA; reverse: AAGGTCTTGGCATTTTCTACAACAG). The analysis utilized the Livak ($2^{-\Delta\Delta C_t}$) method and the results were normalized to the reference gene GAPDH [30].

2.4. Statistical analysis

All experiments were performed in triplicates (metabolic activity, gene expression) or quadruplicates (biochemical assays). Two (biochemical assays, metabolic activity) or three (RT-PCR) measures were acquired per sample. The quantitative assays are reported as mean \pm standard deviation of the replicates (each single point is the average of the 2 or 3 measures for each sample). All statistical tests were performed using IBM SPSS 28.0 software (SPSS Inc.). Comparisons of the different BMP-7 doses and insertion strategies were done using one-way ANOVA. The RT-PCR data were analyzed by the *t*-test. The statistical significance was considered when $p < .05$.

3. Results

3.1. In vitro characterization of cells and cell-seeded hydrogel constructs

Prior to differentiation, we characterized the hMDSCs for expression of the stem cell markers. Indeed, the hMDSCs highly expressed the mesenchymal stem cell markers: CD59 (99.6% of all cells) and CD90 (98.8% of all cells). The hematopoietic and endothelial markers CD45 (2.28% of all cells) and CD34 (2.35% of all cells) [31] were weakly expressed; also, the stem cell growth factor receptor c-kit CD117 was very weakly expressed (2.43% of all cells) (Fig. 2).

The CCK8 assay was performed to evaluate the metabolic activity of the cells cultured on different hydrogels for 14 days. The hMDSCs on CA hydrogel exhibited a significant increase in metabolic activity over the 14 days of culture (* $p < .05$ from d2 to d7; ** $p < .001$ from d7 to d14). For the PEG-CLP-RGD hydrogel, the cells showed a slight increase in metabolic activity from d1 to d14, with no significant increase between the intermediate time points. However, the cell metabolic activity on PEG-CLP constructs significantly decreased at day 7 (** $p < .001$) (Fig. 3, A). Live cell staining showed that the cells were more likely to adhere to the CA hydrogels and the cell shape index showed that the cells were more elongated. Comparing the cells on CA and PEG-CLP-RGD hydrogels at 24 h and 72 h time points, we found a significant difference in the CSI (* $p < .05$ for 24 h and 72 h time points) (Fig. 3, B). After 72 h a dense cell layer was observed spreading over the entire CA hydrogels. Meanwhile, self-aggregated cell clusters were observed on the PEG-CLP-RGD hydrogels (Fig. 3, C–F). Nevertheless, the cell metabolic activity/proliferation showed promising results on CA and PEG-CLP-RGD hydrogels. However, we could conclude that the PEG-CLP hydrogel was not suitable for hMDSC cultivation, as the cells developed a round morphology (data not shown).

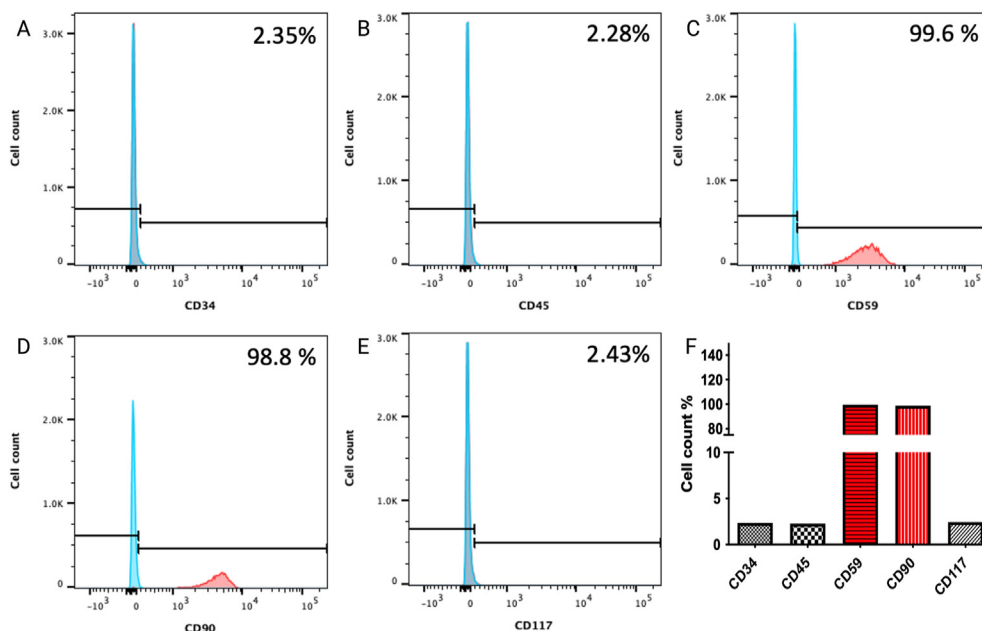


Fig. 2. Expression levels of CD34 (A), CD45 (B), CD59 (C), CD90 (D) and CD117 (E) cell surface markers in hMDSCs. The cells were stained with commercially available fluorochrome-labelled antibodies (red line) and corresponding isotype controls (blue line). The cells highly expressed CD90 and CD59 and were weakly positive for CD34, CD45 and CD117 (F).

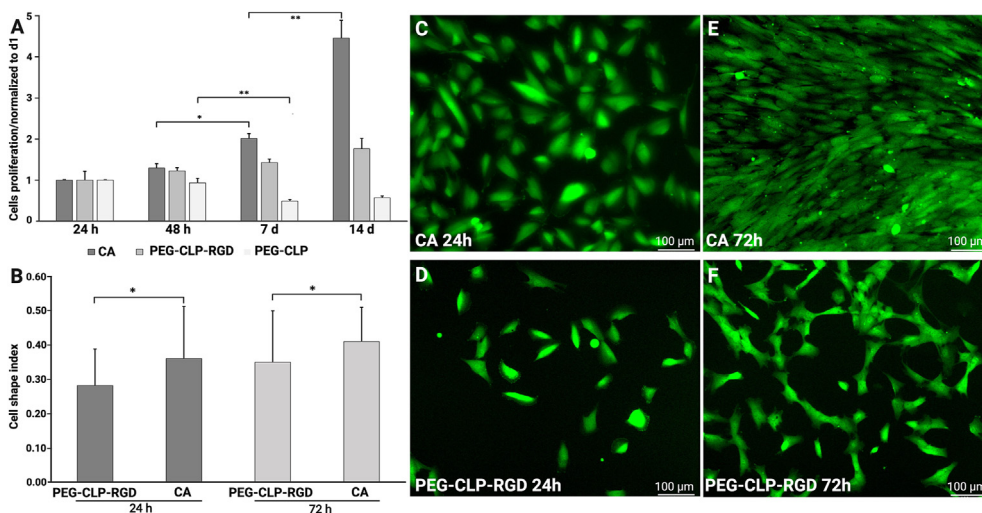


Fig. 3. Proliferation and elongation of hMDSCs on CA, PEG-CLP-RGD and PEG-CLP hydrogels. (A) Cellular metabolic activity (proliferation) assessed with the CCK8 assay (normalized to day 1), * denotes $p < .05$, ** denotes $p < .001$; (B) Cell shape index, $n = 150$, * represents $p < .05$; (C) hMDSCs on CA hydrogel after 24 hours; (D) hMDSCs on PEG-CLP-RGD hydrogel after 24 hours; (E) hMDSCs on CA hydrogel after 72 hours; (F) hMDSCs on PEG-CLP-RGD hydrogels after 72 hours. Scale bar: 100 μm .

3.2. Growth factor loading and release from hydrogels

We first investigated whether adding the GFs - BMP-7 or TGF- β 3 - at different stages of hydrogel crosslinking could lead to improved GF release. As described above, the GFs were incorporated into the hydrogels using three distinct methods: 1) mixing them during the hydrogel casting process, which resulted in the GFs covalently binding to the hydrogel polymers; 2) preparing hydrogel disks that were then resuspended in a “growth factor” buffer, leading to the GFs being encapsulated within the hydrogel; and 3) applying the “growth factor” buffer onto dried hydrogels allowing the GFs to permeate into the hydrogel, thereby suspending them internally.

An important feature of the CA and PEG-CLP-RGD hydrogels is their rapid gelation, facilitating uniform deposition of GFs

throughout the hydrogel's volume. To evaluate the GF release, we monitored BMP-7 diffusion from the hydrogels over a week, using a biochemical ELISA assay. Empty CA and PEG-CLP-RGD hydrogels served as controls (data not shown).

We observed rapid BMP-7 diffusion from the hydrogels immersed in the GF solution, with ~35% of the initially loaded amount released from both the CA and PEG-CLP-RGD hydrogels within the first 24 h. On the other hand, allowing BMP-7 to sink into a dry hydrogel from GF solution was not as effective as expected: only 6 ± 1.7 ng of 75 ng (theoretically) was found in the hydrogels after the experiment. Both strategies for non-crosslinked BMP-7 incorporation (solution and sink-in groups) showed a similar release of BMP-7 within the first 4 h of the experiment as shown by the overlapping release curves (Fig. 4, A). The variation in GF

release, observed after employing different incorporation strategies, may stem from the disparities in initial GF concentrations within the hydrogels post-incorporation and differences in incubation time. Following a 24 h incubation period GF solution, the rate of GF diffusion into and out of the scaffold stabilized, reaching equilibrium. Meanwhile, the sink-in method allowed the unbound GFs to establish weak interactions (e.g. van der Waals) and hydrogen bonds with the scaffold during the drying phase.

In the experimental group where BMP-7 was covalently bound (using mixed-in incorporation strategy), the release of GF from both the CA and PEG-CLP-RGD hydrogels was the lowest. By the conclusion of the one-week experiment, the total amount of BMP-7 released from the hydrogels using mixed-in strategy was $3.68 \pm 1.0\%$ of the initial amount vs $17.75 \pm 2.5\%$ in the case of the sink-in ($p < .05$) and $58 \pm 8.5\%$ using the solution incorporation strategies ($p < .005$) (Fig. 4, A). Despite the higher GF release profile upon incorporation via the solution technique, for further experiments we chose the sink-in strategy.

We found that the sink-in incorporation strategy allowed a sustained release of TGF- β 3: $6.0 \pm 0.3\%$ of the initially loaded amount diffused out after 4 h from the CA and PEG-CLP-RGD hydrogels. For BMP-7, $13.1 \pm 2.3\%$ and $15.75 \pm 1.6\%$ of the initially loaded amount diffused out after 4 h, respectively (Fig. 4, B).

Since the exact amount of a specific GF within the hydrogel at the start of differentiation is unknown, we chose to investigate minimal dosages. This approach leverages the inherent capabilities of both hydrogel types to retain and subsequently release GFs into the cell culture media. For our experiments across different GF incorporation strategies, we utilised 75 ng of BMP-7 per scaffold. In the next phase, we tracked the diffusion GFs from the CA and PEG-CLP-RGD hydrogels over two weeks by regularly changing the cell culture medium. We observed almost identical diffusion of the GFs from the hydrogels containing different amount of the initially loaded TGF- β 3 (100 and 75 ng/hydrogel) and BMP-7 (150, 100 and 75 ng/hydrogel). We could see a significant difference in GF release in the 150 ng/hydrogel experimental group and observed a burst release pattern (Fig. 4, C). No notable differences were observed in

the release patterns between TGF- β 3 and BMP-7 (the TGF- β 3 data not shown).

The release patterns of GFs were monitored for hydrogels loaded with both BMP-7 and TGF- β 3, at 75 ng of each growth factor per hydrogel. Previous experiments demonstrated more effective release of BMP-7 from both hydrogel types compared to TGF- β 3. The release pattern did not change significantly: we could observe a higher release of BMP-7 and a lower release of TGF- β 3. Only $3.4 \pm 0.9\%$ of the initially loaded TGF- β 3 amount diffused out after 4 h and only $8.3 \pm 1.7\%$ got released after 14 days (Fig. 4, D). Collectively, our experimental findings indicate that BMP-7 and TGF- β 3 copolymer formation with CA and PEG-CLP-RGD hydrogels is an effective strategy for developing cartilage tissue engineering systems. Consequently, we have adopted these biomaterials as platforms for *in vitro* chondrogenesis screening.

3.3. Characterization hMDSCs proliferation on GF-loaded hydrogels under different oxygen conditions

We characterized hMDSC proliferation on the hydrogels with the inserted growth factors and determined how cell proliferation changes under different oxygen (21% vs 1%) conditions. We observed a similar DNA fold change (3.6 ± 0.33 in normoxia vs 3.19 ± 0.32 in hypoxia) on the CA hydrogels (Fig. 5, A). Under normoxia, the insertion of GFs into the hydrogels led to a decreased proliferation rate, with scaffolds containing TGF- β 3 showing a higher proliferation rate ($p < .05$). Under hypoxia, the proliferation rate on hydrogels with the inserted GFs increased significantly, except for the CA/TGF- β 3 (3.05 ± 0.33 in normoxia vs 3.03 ± 0.53 in hypoxia) (Fig. 5, B). Meanwhile, the proliferation rates on the PEG-CLP-RGD hydrogels with inserted GFs did not change significantly under normoxia and significantly higher DNA fold change (3.43 ± 0.57) was observed on positive control scaffolds (Fig. 5, C). The proliferation rates decreased for all PEG-CLP-RGD hydrogels under hypoxic conditions (Fig. 5, D).

Consequently, we concluded that adding GFs to CA and PEG-CLP-RGD hydrogels can influence cell proliferation rates in

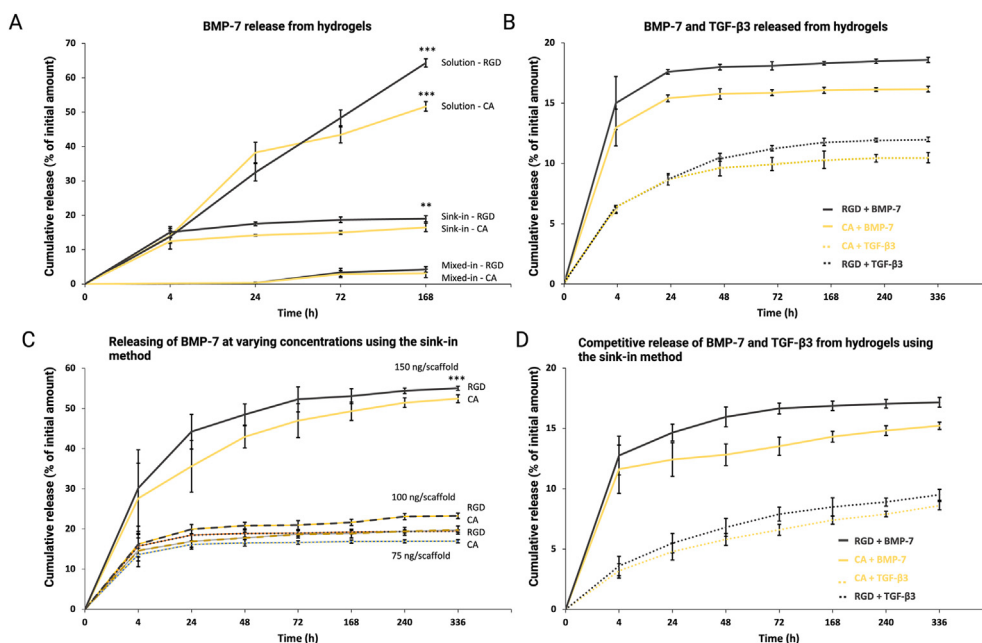


Fig. 4. Cumulative release of BMP-7 and TGF- β 3 from hydrogels. (A) BMP-7 release after using different GF insertion strategies, ** denotes $p < .05$, *** $p < .005$; (B) BMP-7 and TGF- β 3 release from CA and PEG-CLP-RGD hydrogels over 2 weeks using sink-in strategy; (C) BMP-7 release after using different GF loading concentrations, *** denotes $p < .005$; (D) BMP-7 and TGF- β 3 cumulative release from the same hydrogel.

varying directions. The CA hydrogels alone had a more pronounced impact on proliferation, whereas the PEG-CLP-RGD scaffolds were more neutral, not significantly affecting proliferation rates.

3.3.1. hMDSC chondrogenesis on CA hydrogels under normoxia and hypoxia

Following the observed proliferation behavior of the hMDSCs on the CA and PEG-CLP-RGD hydrogels loaded with GFs, we further investigated the efficiency of the constructs to stimulate chondrogenesis *in vitro*. As markers of chondrogenesis we chose and measured the gene expression of *COL1A1*, *ACAN*, and *VCAN*. For determination of cartilaginous ECM production, we estimated GAG and collagen type II deposition.

Under the normal oxygen conditions, collagen type I was significantly more expressed in the positive control group using CA/PC scaffolds compared to other experimental groups ($p < .001$ for all CA scaffolds with the GFs or alone). Interestingly, the CA scaffold alone did not show an increased collagen type I expression as expected with regard to enhanced proliferation results (1.05 ± 0.17 times compared to *GAPDH*). We observed a decrease of collagen type I gene expression on hydrogels loaded with BMP-7 (0.58 ± 0.21) (Fig. 6, A). Experimental TGF- β 3 group yielded the highest Col I expression compared to the hydrogels loaded with GFs ($p < .05$). Aggrecan gene expression did not follow the same trend as collagen type I. Instead, aggrecan expression in the positive control group was significantly lower compared to the CA scaffolds with GFs or the unmodified ones ($p < .005$ for CA/B+T and CA/T, $p < .05$ for CA and CA/B). Moreover, *ACAN* expression on the CA/B+T and CA/T scaffolds was significantly higher compared to the CA hydrogel

loaded with BMP-7 and CA hydrogel alone ($p < .005$) (Fig. 6, B). The aggrecan/versican (*ACAN/VCAN*) gene expression ratio is an index of differentiation or dedifferentiation of chondrocytes; therefore, we calculated this ratio to determine the differentiation index of the hMDSCs. The obtained results revealed a higher index on the scaffolds with inserted growth factors (Fig. 6, C). And the CA/B+T and CA/T scaffolds displayed a significantly higher ratio compared to the CA and CA/B ($p < .05$) and positive control groups, respectively ($p < .005$). It is particularly important to note that scaffolds with BMP-7 insertion exhibited a higher differentiation ratio compared to the CA scaffolds alone ($p < .05$), as aggrecan gene expression was smaller than that seen for the CA hydrogel.

Furthermore, the deposition of collagen type II and GAGs was consistent with the results of the *ACAN/VCAN* differentiation index. Col II secretion was detected in all experimental groups, with the highest expression observed in scaffolds containing both growth factors. However, no significant differences were found between the various GF groups (Fig. 6, D). Similarly, the GAGs measurements followed the same pattern, with the exception that CA hydrogels containing GFs showed more GAG deposition compared to those in the positive control group (Fig. 6, E).

Given that hypoxia positively affects the healthy chondrocyte phenotype and ECM formation, we investigated its impact on hMDSC chondrogenic differentiation. The highest expression of *COL1A1* was observed in the positive control CA hydrogels, significantly surpassing that in the other CA scaffolds, whether loaded with GFs or unmodified ($p < .001$) (Fig. 6, A). Interestingly, under hypoxic conditions, collagen type I expression in the positive control group was reduced by two-fold compared to normal

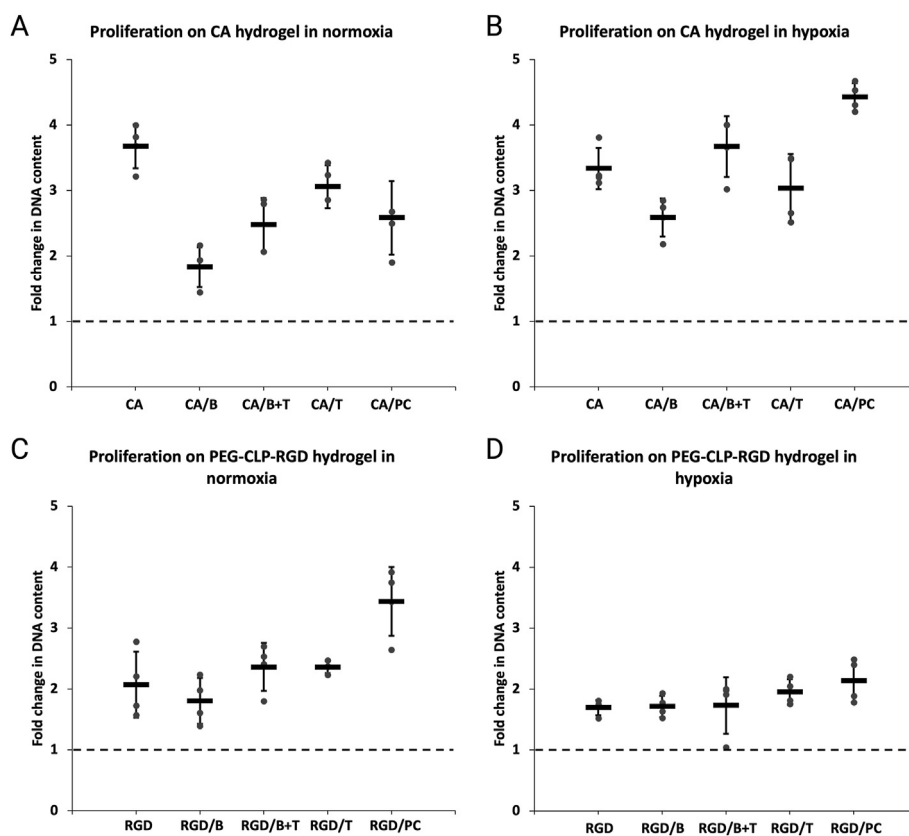


Fig. 5. Characterization of hMDSC proliferation on hydrogels loaded with growth factors investigated under normal oxygen and hypoxia conditions for 28 days and measured by estimating fold change in DNA content; (A) hMDSCs on CA hydrogels after 28 days under normal oxygen conditions; (B) hMDSCs on CA hydrogel after 28 days in hypoxic conditions; (C) hMDSCs on PEG-CLP-RGD hydrogel after 28 days under normal oxygen conditions; (D) hMDSCs on PEG-CLP-RGD hydrogel after 28 days in hypoxia. B - BMP-7, B+T - BMP-7+TGF- β 3, T - TGF- β 3, PC - positive control, chondrogenic medium.

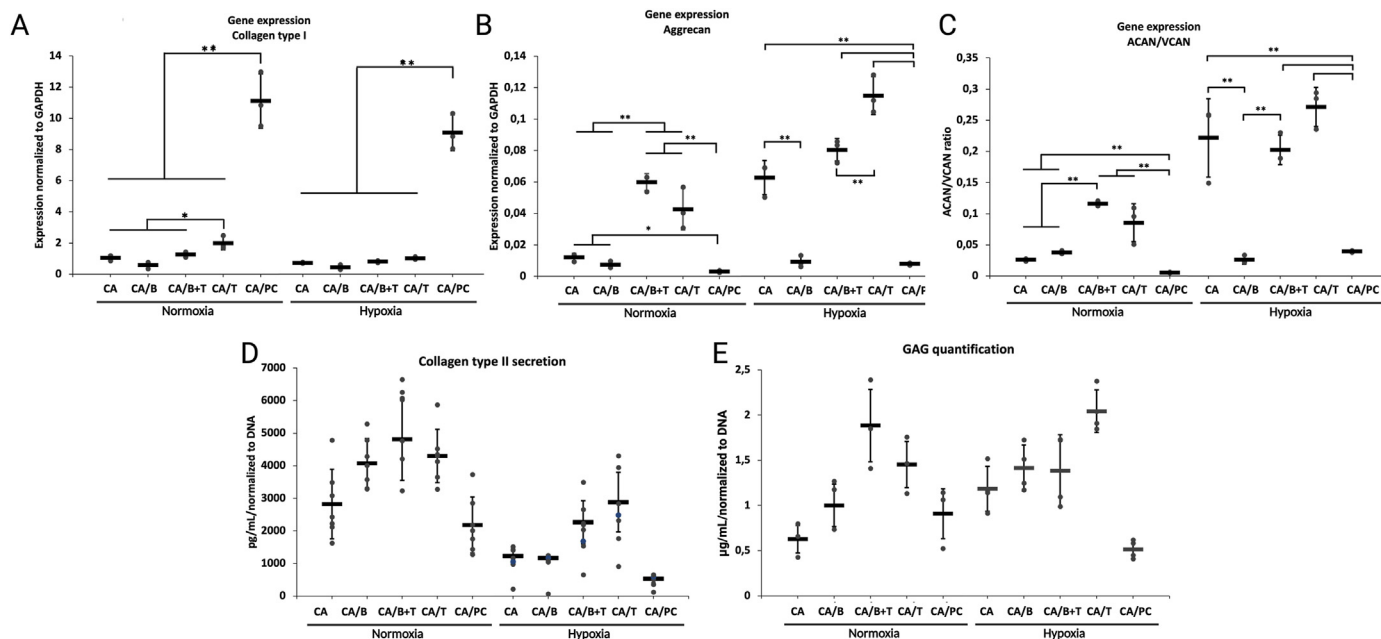


Fig. 6. hMDSCs chondrogenic differentiation on the CA hydrogels under normal oxygen conditions and hypoxia. (A) Collagen type I expression normalized to GAPDH at d28; (B) Aggrecan gene expression normalized to GAPDH at d28; (C) Aggrecan and versican gene expression ratio at d28; (D) Collagen type II deposition normalized to DNA at d28; (E) GAG deposition at d28. B - BMP-7, T - TGF-β3, PC - chondrogenic differentiation medium; * represents $p < .05$, ** represents $p < .005$, *** represents $p < .001$.

conditions. Under hypoxic conditions, *ACAN* expression was significantly higher in TGF-β3 loaded hydrogels ($p < .005$ for CA/PC and CA/B, $p < .05$ for CA/B+T and CA alone) (Fig. 6, B). Moreover, a significant increase of aggrecan expression was observed for the CA hydrogel alone (6-folds compared to the CA hydrogel under normoxia). Hypoxia conditions did not have any effect in the case of CA hydrogels loaded with BMP-7 (Fig. 6, B). Also, the *ACAN/VCAN* ratio followed same pattern as aggrecan gene expression. Surprisingly, differentiation ratio for CA scaffolds was not significantly different compared to CA/B+T and CA/T. Moreover, it was 10-fold higher than under normoxia (Fig. 6, C).

ECM production under hypoxia was significantly decreased compared to the normoxia. Moreover, Col II deposition was the same on the CA alone and CA/B scaffolds (Fig. 6, D). And GAGs quantification showed higher GAG deposition on CA, CA/B+T and CA/T scaffolds, in contrast to the lowest deposition on CA hydrogels loaded with BMP-7 (Fig. 6, E).

3.3.2. hMDSCs chondrogenesis on PEG-CLP-RGD hydrogels under normoxia and hypoxia

Similar Col I expression levels were detected on PEG-CLP-RGD hydrogels as on CA hydrogels. Collagen type I expression was significantly higher in the control group compared to the PEG-CLP-RGD scaffolds loaded with GFs or PEG-CLP-RGD hydrogels alone ($p < .001$) (Fig. 7, A). Interestingly, the presence of the different GFs in the scaffolds did not influence collagen type I gene expression. Meanwhile, aggrecan core protein gene expression in the positive control group was significantly lower compared to the scaffolds with or without GFs ($p < .005$) (Fig. 7, B). The scaffolds loaded with BMP-7 displayed a lower aggrecan expression than the scaffolds with TGF-β3 or BMP-7/TGF-β3. This pattern was visible for the CA/BMP-7 hydrogels as well. Surprisingly, aggrecan expression on the PEG-CLP-RGD scaffold alone was not significantly different as compared to the scaffold loaded with both GFs. The differentiation ratios (*ACAN/VCAN*) followed the same pattern as *ACAN* gene expression.

The production of ECM by the cells on the PEG-CLP-RGD hydrogels was lower compared to the CA hydrogels under normoxia. The hydrogels of BMP-7/TGF-β3 in the PEG-CLP-RGD scaffolds resulted in highest Col II deposition, but it was not significantly meaningful comparing to the same scaffolds loaded with TGF-β3 (Fig. 7, D). Interestingly, the total amount of GAGs in the hydrogels loaded with the GFs was significantly lower compared to the PEG-CLP-RGD hydrogel alone or positive control hydrogel ($p < .005$ from scaffolds loaded with GFs, $p < .05$ from PEG-CLP-RGD/PC) (Fig. 7, D). We found no significant difference between the scaffolds loaded with GFs. Furthermore, GAG quantification in the PEG-CLP-RGD hydrogel group diverged from the pattern noted for the CA hydrogels under identical conditions.

Hypoxia did not significantly change Col I expression pattern for the PEG-CLP-RGD hydrogel compared to normoxia (Fig. 7, A). Interestingly, for the first time PEG-CLP-RGD scaffolds loaded with BMP-7 growth factor showed slightly higher gene expression rate (no significant difference) compared to PEG-CLP-RGD scaffolds alone or scaffolds with GFs inserted. Collagen type I expression in the chondrogenic medium group decreased nearly threefold compared to conditions of normal oxygen (Fig. 7, A). Aggrecan expression was significantly higher in scaffolds loaded with GFs and those consisting of PEG-CLP-RGD alone, when compared to the positive control group ($p < .005$). The *ACAN/VCAN* index was elevated on hydrogels containing GFs. When compared to normoxic conditions, the *ACAN/VCAN* ratio for PEG-CLP-RGD/B hydrogels doubled under hypoxia. Conversely, it decreased for the PEG-CLP-RGD/B+T and PEG-CLP-RGD/T scaffolds (Fig. 7, C). Unexpectedly, Col II deposition on PEG-CLP-RGD hydrogels was very low and no significant differences were observed across all experimental groups (Fig. 7, D). In contrast, GAG deposition presented quite opposite results: it significantly increased in all experimental groups, with the exception of the positive control group (Fig. 7, B).

The summarized results of changes in gene expression and protein secretion in cells on CA and PEG-CLP-RGD hydrogels, either containing GFs or used unmodified, are presented in Table 1.

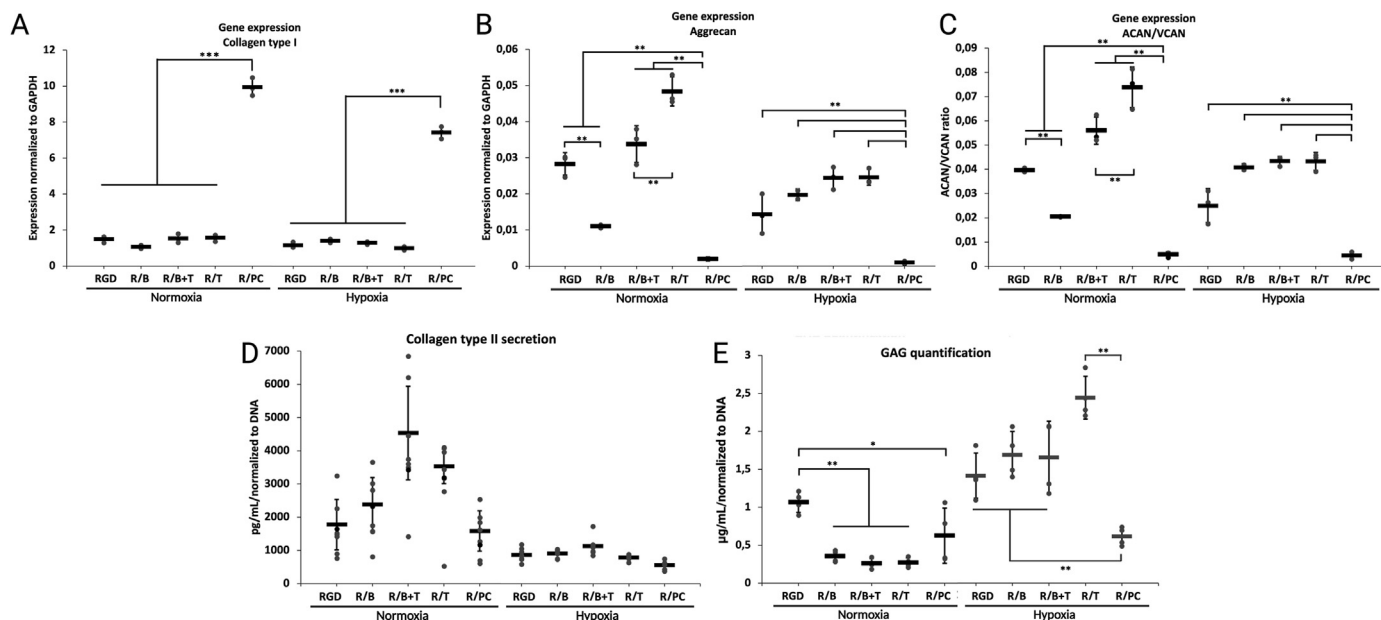


Fig. 7. hMDSCs chondrogenic differentiation on PEG-CLP-RGD hydrogels under normal oxygen conditions and hypoxia. (A) Collagen type I expression normalized to GAPDH at d28; (B) Aggrecan gene expression normalized to GAPDH at d28; (C) Aggrecan and versican genes expression ratio at d28; (D) Collagen type II deposition normalized to DNA at d28; (E) GAG deposition at d28. B - BMP-7, T - TGF-β3, PC - chondrogenic differentiation medium; * denotes $p < .05$, ** denotes $p < .005$, *** denotes $p < .001$.

4. Discussion

In this manuscript, we have successfully incorporated TGF-β3 and BMP-7 growth factors into the self-supporting hydrogels under investigation, assessing their chondrogenic potential *in vitro*. These constructs enabled us to examine the effects of GFs on hMDSC chondrogenic differentiation. To mitigate any negative effects from GF release, we conducted our assays using acellular hydrogels. Meanwhile, for chondrogenesis studies, we utilized hydrogels seeded with cells. Consequently, ELISA results cannot fully predict the extent of chondrogenesis, given that cells respond differently based on the availability of GFs such as TGF-β3 and BMP-7. This response includes effects from GF internalization upon binding and GF activity mediated through receptor internalization. For GF incorporation, we employed three distinct strategies: mixing during the hydrogel casting process, resuspension in a GF solution, and sink-in protocol. Moreover, combining both GFs in same hydrogel altered their release profiles, notably slowing TGF-β3's release. Although we found no statistically significant difference in GF release between CA and PEG-CLP-RGD scaffolds overall, differences in the amounts of specific growth factors released were noted. Importantly, GFs differ from other oligo-/polypeptide molecules in their delivery mode and the responses they elicit. They typically diffuse over short-ranges through the extracellular matrix and act locally, due to their short half-lives and slow diffusion rates. In the CA and PEG-CLP-RGD hydrogels, the absence of heparin-binding domains, which are key for mediating specific interactions with the ECM, is noteworthy. Structurally, the CA and PEG-CLP-RGD hydrogels are similar: both contain the triple helix-forming amino acid sequences. Therefore, the total amount of hydrogen-bond donor groups per volume is expected to be rather similar (note that the PEG-CLP-RGD hydrogels also contain up to 60% of PEG). Thus, we speculate that observed differences in the GF release profiles may stem from the distinct molecular masses of the amino acid sequences, conformations, and other molecular characteristics of the GFs. Interestingly, despite its higher molecular mass (38 kDa for BMP-7 vs. 26 kDa for TGF-β3), the cumulative release of BMP-7 was

greater than that of TGF-β3. This phenomenon may be attributed to slower reverse trapping of BMP-7 by the hydrogels, leading to its enhanced release. Such findings have implications for the behavior of hMDSCs in cartilage tissue formation. Furthermore, the slower and more sustained release of TGF-β3, especially when both growth factors are inserted, are the desirable traits that could significantly affect cell behavior.

Moreover, to stimulate chondrogenic differentiation, appropriate auxiliary conditions such as hypoxia, hydrostatic pressure, and compressive force can be applied [32,33]. In our study we opted for severe hypoxia conditions (1%) to explore this further. Initially, we examined the impact of GF loading and varying oxygen conditions on hMDSC proliferation. As anticipated, the highest proliferation rate was observed with CA hydrogels under normal oxygen conditions and without GFs, yet hypoxia did not inhibit cell proliferation on these hydrogels. In contrast, for PEG-CLP-RGD hydrogels, hypoxia consistently inhibited hMDSC proliferation across all experimental groups. Cartilaginous cells can survive in inhospitable hypoxic environments, a capability attributed to HIF-1α. This factor promotes the expression of chondrogenic genes (*SOX-9*, *COL2A1* and *ACAN*) and facilitates matrix formation [34]. Specifically, with collagen type I hydrogels, cells can adhere to the hydrogel surface via various integrins. Although the synthetic hydrogel contains the sequence necessary for forming a triple-helix structure and includes the RGD cell-binding domain, interactions between cells and PEG-CLP-RGD occur directly only through the α5β1 or αVβ3 integrins. In the native conformation of collagen I, the RGD-motifs are inaccessible to RGD-binding integrins; only through thermal or proteolytic denaturation, which unwinds the triple-helical structure, are RGD-motifs exposed [35,36]. As CA hydrogel is composed of collagen in its native conformation, its RGD-motifs cannot be recognised by cell integrins. Gene expression profiles indicate that, within the first week of differentiation, human mesenchymal stem cells upregulate fibronectin production, which provides an adhesive site for cell condensation, cell signaling and eventually the early stages of chondrogenic differentiation [37,38]. In our experiments with PEG-CLP-RGD hydrogels, we

Table 1
The summary of the hMDSC chondrogenic differentiation results in each experimental group: hydrogel type, inserted growth factor, difference in gene expression and protein secretion comparing to hydrogel without growth factors under normal and hypoxic oxygen conditions.

Hydrogel type	GF	21% O ₂ (normoxia)					1% O ₂ (hypoxia)				
		Gene expression			Protein secretion		Gene expression			Protein secretion	
		COL1A1	ACAN	ACAN/VCAN	Col II	GAGs	COL1A1	ACAN	ACAN/VCAN	Col II	GAGs
CA	BMP-7	=	↓	↑	↑	↑	↓	↓	↓	=	=
	B+T	=	↑	↑	↑	↑	↑	↑	=	↑	=
	TGF-β3	↑	↑	↑	↑	↑	↑	↑	=	↑	↑
	PC	↑	↓	↓	↓	↑	↑	↓	↓	↓	↓
PEG-CLP-RGD	BMP-7	=	↓	↓	=	↓	=	=	↑	=	=
	B+T	=	=	=	↑	↓	=	=	↑	=	=
	TGF-β3	=	↑	↑	↑	↓	=	=	↑	=	↑
	PC	↑	↓	↓	=	↓	↑	↓	↓	=	↓

↑ - Increase compared to hydrogel without GFs
 ↓ - Decrease compared to hydrogel without GFs
 = - No significance difference compared to hydrogel without GFs

observed the formation of self-aggregated cell clusters as early as day 3. Integrin recognition of RGDs on the hydrogel surface could cause cell condensation and inhibit proliferation because of the ability of the signals to induce chondrogenesis at the very beginning of the experiments under both oxygen conditions.

In vitro culture, being time-bound, allows gene expression data to reveal insights into cell behavior at harvest time and the maturation process of constructs. Chondrogenic differentiation *in vitro* is characterized by both genotypic and phenotypic manifestations of specific cartilage markers. In this study, we analyse the expression of COL1A1, ACAN, and VCAN genes, along with the deposition of Col II and GAGs, following 28 days of culturing hMDSCs in both growth medium and chondrogenic differentiation medium. In all experimental groups cultured in basal cell culture medium, collagen type I expression on both CA and PEG-CLP-RGD hydrogels did not significantly differ. Under the normoxic conditions, CA hydrogels containing both GFs exhibited the highest levels of GAGs levels and Col II deposition. Notably, Col II secretion in both CA and PEG-CLP-RGD hydrogels under these conditions exceeded that observed in the positive control group. Our results validate the hypothesis that the hydrogel alone can promote chondrogenesis. While BMP-7 alone could not influence chondrogenic differentiation, TGF-β3 showed very similar results to the dual growth factor experimental group. Notably, hypoxia further enhanced chondrogenic differentiation in the TGF-β3 group, with aggrecan expression and GAG deposition both nearly tripling. However, it intriguingly led to a reduction in collagen type II secretion. Interestingly, under normoxic conditions, the quantity of GAGs on PEG-CLP-RGD hydrogels was significantly lower compared to that under hypoxia. Additionally, the ACAN/VCAN ratio and ACAN gene expression were higher in the PEG-CLP-RGD/BMP-7 and PEG-CLP-RGD/TGF-β3 groups under normoxia, whereas Col II deposition was notably lower in the constructs under hypoxia. Our explanation is that the differences in protein secretion may occur because of different signaling of GFs or due to severe hypoxia itself. According to existing studies, TGFβ signaling induces the SMAD2/3 pathway, whereas BMP signalling triggers SMAD1/5/9 [39,40]. Activation of SMAD2/3 pathway is associated with anti-hypertrophic and anti-inflammatory effects, characterised by the upregulation of the SOX9 transcription factor and the

downregulation of RUNX2. Conversely, SMAD1/5/9 signaling is associated with pro-hypertrophic regulation of the ECM and maturation of the cartilage (both SOX9 and RUNX2 are upregulated). Meanwhile, under hypoxia conditions, the HIF-1α enhance BMP-2-induced chondrogenic differentiation via interactions with SOX9 to up-regulate COL2A1 and ACAN genes and downregulate RUNX2 expression. Therefore, BMP-2 and BMP-7 could downregulate each other through a negative feedback mechanism. This might account for the observed Col II deposition decrease on the CA hydrogels. On the other hand, in all experimental groups, we observed a decrease in collagen II deposition on the PEG-CLP-RGD hydrogels, while synthesis of non-collagenous protein (such as GAGs and aggrecan) did not show any significant reduction. This indicates that TGF-β3 signaling - whether alone or in combination with BMP-7 - was the only factor able to promote Col II deposition under hypoxia. Conversely, hypoxia appeared to suppress collagenous protein synthesis on the PEG-CLP-RGD hydrogels. Numerous studies have shown that hypoxia may enhance expression of some chondrogenic markers during the differentiation phase [41–45]. However, Cicione et al. found that severe hypoxia actually inhibits chondrogenesis, with increased ACAN and COL1A1 gene expression in normoxia, but a notable absence of collagens and proteoglycans under hypoxic conditions [45]. Contrary to these findings, our results demonstrated lower ACAN gene expression on CA hydrogels and increased expression on PEG-CLP-RGD hydrogels following TGF-β3 release under normal oxygen conditions. Neybecker et al. also found that chondrogenic differentiation markers could be upregulated at the gene level but not at the protein level [44]. In our experiments, collagen secretion was significantly reduced on CA hydrogels and nearly inhibited on PEG-CLP-RGD hydrogels under hypoxia, despite the presence of GFs.

5. Conclusion

In summary, we have shown that CA and PEG-CLP-RGD scaffolds, when loaded with BMP-7 and TGF-β3, effectively stimulated the differentiation of hMDSCs into cartilage-like tissue *in vitro*, both under normal and low oxygen conditions. The key findings include: i) hydrogels themselves can stimulate hMDSC chondrogenesis

in vitro by inducing gene expression of cartilage-specific proteoglycan aggrecan and ECM production; ii) the combined effect of BMP-7 and TGF- β 3 loading was more pronounced on CA hydrogels under normal oxygen levels; iii) on PEG-CLP-RGD hydrogels, dual growth factor loading did not show an additive effect, with TGF- β 3 alone being more effective under both oxygen conditions; iv) BMP-7 enhanced the chondrogenic impact of TGF- β 3 on CA scaffolds, demonstrating that hydrogels loaded with both growth factors can induce cartilage formation in hMDS cell cultures. Collectively, these results indicate that CA hydrogels provide a more natural microenvironment for chondrogenesis. However, the functional PEG-CLP-RGD mimetic peptide hydrogel also holds a promise as a future carrier for delivering hMDS cells to damaged cartilage areas for repair. This study underscores the potential of self-supporting, chemically crosslinked hydrogels as viable substrates for autologous human muscle-derived stem cell therapy.

Author contribution

A.M-G, A.U – conception and design. A. V., T. J. – hydrogel preparation. A. M-G. – hMDS isolation. J. D. – flow cytometry measurements, data analysis. A. M-G. – *in vitro* experiments, protein binding, data analysis. A. M-G. – manuscript drafting. A. M-G., A. U. – manuscript editing. All authors have read and agreed to the published version of the manuscript.

Role of funding source

This work was supported by Lithuanian University of Health Sciences Department of Research Affairs Foundation.

Acknowledgements

The authors would like to thank Dr. Ramūnas Valiokas for suggestions on the study design and scientific input, Dr. Lina Jankauskaitė for the first batch of hMDS, Romuald Eimont and Dr. Vytautas Čepėla for sharing knowledge of hydrogel characterization, Dr. Arvydas Kanopka for the technical help with hypoxia experiments.

References

- Makris EA, Gomoll AH, Malizos KN, Hu JC, Athanasiou KA. Repair and tissue engineering techniques for articular cartilage. *Nat Rev Rheumatol* 2015;11(1): 21–34. <https://doi.org/10.1038/nrrheum.2014.157>.
- Makris EA, Gomoll AH, Malizos KN, Hu JC, Athanasiou KA. Repair and tissue engineering techniques for articular cartilage. *Nat Rev Rheumatol* 2015;11(1): 21–34. <https://doi.org/10.1038/nrrheum.2014.157>.
- Fu L, Guo W, Guo Q. Editorial: biomaterial advances in cartilage and meniscus regeneration. *Front Bioeng Biotechnol* 2022;10. <https://doi.org/10.3389/fbioe.2022.1054268>.
- Wasyleczko M, Sikorska W, Chwojnowski A. Review of synthetic and hybrid scaffolds in cartilage tissue engineering. *Membranes* 2020;10(11):1–28. <https://doi.org/10.3390/membranes10110348>.
- Chinta ML, Velidandi A, Pabbathi NPP, Dahariya S, Parcha SR. Assessment of properties, applications and limitations of scaffolds based on cellulose and its derivatives for cartilage tissue engineering: a review. *Int J Biol Macromol* 2021;175:495–515. <https://doi.org/10.1016/j.ijbiomac.2021.01.196>.
- Patel JM, Saleh KS, Burdick JA, Mauck RL. Bioactive factors for cartilage repair and regeneration: improving delivery, retention, and activity. *Acta Biomater* 2019;93:222–38. <https://doi.org/10.1016/j.actbio.2019.01.061>.
- Fan H, Tao H, Wu Y, Hu Y, Yan Y, Luo Z. TGF- β 3 immobilized PLGA-gelatin/chondroitin sulfate/hyaluronic acid hybrid scaffold for cartilage regeneration. *J Biomed Mater Res* 2010;95(4):982–92. <https://doi.org/10.1002/jbm.a.32899>.
- Yang J, Zhang YS, Yue K, Khademhosseini A. Cell-laden hydrogels for osteochondral and cartilage tissue engineering. *Acta Biomater* 2017;57:1–25. <https://doi.org/10.1016/j.actbio.2017.01.036>.
- Jankauskaite L, Malinauskas M, Aukstikalne L, Dabasiuskaite L, Rimkunas A, Micekevicius T, et al. Functionalized electrospun scaffold–human-muscle-derived stem cell construct promotes *in vivo* neocartilage formation. *Polymers* 2022;14(12). <https://doi.org/10.3390/polym14122498>.
- Maehara H, Sotome S, Yoshii T, Torigoe I, Kawasaki Y, Sugata Y, et al. Repair of large osteochondral defects in rabbits using porous hydroxyapatite/collagen (HAp/Col) and fibroblast growth factor-2 (FGF-2). *J Orthop Res* 2010;28(5): 677–86. <https://doi.org/10.1002/jor.21032>.
- Nakagawa Y, Fortier LA, Mao JJ, Lee CH, Goodale MB, Koff MF, et al. Long-term evaluation of meniscal tissue formation in 3-dimensional-Printed scaffolds with sequential release of connective tissue growth factor and TGF- β 3 in an ovine model. *Am J Sports Med* 2019;47(11):2596–607. <https://doi.org/10.1177/0363546519865513>.
- González-Gómez P, Anselmo NP, Mira H. BMPs as therapeutic targets and biomarkers in astrocytic glioma. *BioMed Res Int* 2014;2014. <https://doi.org/10.1155/2014/549742>.
- Crecente-Campo J, Borrajo E, Vidal A, Garcia-Fuentes M. New scaffolds encapsulating TGF- β 3/BMP-7 combinations driving strong chondrogenic differentiation. *Eur J Pharm Biopharm* 2017;114:69–78. <https://doi.org/10.1016/j.ejpb.2016.12.021>.
- Yu X, Zhang H, Miao Y, Xiong S, Hu Y. Recent strategies of collagen-based biomaterials for cartilage repair: from structure cognition to function endowment. *J Leather Sci Eng* 2022;4(1). <https://doi.org/10.1186/s42825-022-00085-4>.
- Pustlank W, Paul B, Gelinsky M, Bernhardt A. Jellyfish collagen and alginate: combined marine materials for superior chondrogenesis of hMSC. *Mater Sci Eng C* 2016;64:190–8. <https://doi.org/10.1016/j.msec.2016.03.081>.
- Wu Z, Korntner SH, Mullen AM, Zeugolis DI. In the quest of the optimal chondrichthyan for the development of collagen sponges for articular cartilage. *J Sci Adv Mater* 2021;6(3):390–8. <https://doi.org/10.1016/j.jsamd.2021.04.002>.
- Kudva AK, Luyten FP, Patterson J. RGD-functionalized polyethylene glycol hydrogels support proliferation and *in vitro* chondrogenesis of human periosteum-derived cells. *J Biomed Mater Res* 2018;106(1):33–42. <https://doi.org/10.1002/jbm.a.36208>.
- Tao T, Li Y, Gui C, Ma Y, Ge Y, Dai H, et al. Fibronectin enhances cartilage repair by activating progenitor cells through integrin α 5 β 1 Receptor. *Tissue Eng* 2018;24(13–14):1112–24. <https://doi.org/10.1089/ten.tea.2017.0322>.
- Deasy BM, Gharaibeh BM, Pollett JB, Jones MM, Lucas MA, Kanda Y, et al. Long-term self-renewal of postnatal muscle-derived stem cells. *Mol Biol Cell* 2005;16(7):3323–33. <https://doi.org/10.1091/mbc.E05-02-0169>.
- Malinauskas M, Jankauskaite L, Aukstikalne L, Dabasiuskaite L, Rimkunas A, Micekevicius T, et al. Cartilage regeneration using improved surface electrospun bilayer polycaprolactone scaffolds loaded with transforming growth factor-beta 3 and rabbit muscle-derived stem cells. *Front Bioeng Biotechnol* 2022;10. <https://doi.org/10.3389/fbioe.2022.971294>.
- Thoms BL, Dudek KA, Lafont JE, Murphy CL. Hypoxia promotes the production and inhibits the destruction of human articular cartilage. *Arthritis Rheum* 2013;65(5):1302–12. <https://doi.org/10.1002/art.37867>.
- Ranmuthu CKI, Ranmuthu CDS, Wijewardena CK, Seah MKT, Khan WS. Evaluating the effect of hypoxia on human adult mesenchymal stromal cell chondrogenesis *in vitro*: a systematic review. *Int J Mol Sci* 2022;23(23). <https://doi.org/10.3390/ijms232315210>.
- Islam MM, Ravichandran R, Olsen D, Ljunggren MK, Fagerholm P, Lee CJ, et al. Self-assembled collagen-like-peptide implants as alternatives to human donor corneal transplantation. *RSC Adv* 2016;6(61):55745–9. <https://doi.org/10.1039/c6ra08895c>.
- Balio Z, Čepėla V, Svirskiene N, Svirskis G, Druceikaite K, Inokaitis H, et al. Cerebellar cells self-assemble into functional organoids on synthetic, chemically crosslinked ECM-mimicking peptide hydrogels. *Biomolecules* 2020;10(5). <https://doi.org/10.3390/biom10050754>.
- Balio Z, Sipailaitė E, Stasyte G, Vaillionyte A, Mazetyte-Godiene A, Seskeviciute I, et al. Investigation of cancer cell migration and proliferation on synthetic extracellular matrix peptide hydrogels. *Front Bioeng Biotechnol* 2020;2020:8. <https://doi.org/10.3389/fbioe.2020.00773>.
- Islam MM, Buznyk O, Reddy JC, Pasychchnikova N, Alarcon EI, Hayes S, et al. Biomaterials-enabled cornea regeneration in patients at high risk for rejection of donor tissue transplantation. *NPJ Regen Med* 2018;3(1). <https://doi.org/10.1038/s41536-017-0038-8>.
- Liu Y, Gan L, Carlsson DJ, Fagerholm P, Lagali N, Watsky MA, et al. A simple, cross-linked collagen tissue substitute for corneal implantation. *Invest Ophthalmol Vis Sci* 2006;47(5):1869–75. <https://doi.org/10.1167/iov.05-1339>.
- Lavasan M, Lu A, Thompson SD, Robbins PD, Huard J, Niedernhofer LJ. Isolation of muscle-derived stem/progenitor cells based on adhesion characteristics to collagen-coated surfaces. *Methods Mol Biol* 2013;976:53–65. https://doi.org/10.1007/978-1-62703-317-6_5.
- Levinson C, Lee M, Applegate LA, Zenobi-Wong M. An injectable heparin-conjugated hyaluronan scaffold for local delivery of transforming growth factor β 1 promotes successful chondrogenesis. *Acta Biomater* 2019;99: 168–80. <https://doi.org/10.1016/j.actbio.2019.09.017>.
- Livak KJ, Schmittgen TD. Analysis of relative gene expression data using real-time quantitative PCR and the 2- $\Delta\Delta$ CT method. *Methods* 2001;25(4):402–8. <https://doi.org/10.1006/meth.2001.1262>.
- Sidney LE, Branch MJ, Dunphy SE, Du HS, Hopkinson A. Concise review: evidence for CD34 as a common marker for diverse progenitors. *Stem Cell* 2014;32(6):1380–9. <https://doi.org/10.1002/stem.1661>.
- Jahangir S, Eglin D, Pötter N, Ravani MK, Stoddart MJ, Samadikuchaksare A, et al. Inhibition of hypertrophy and improving chondrocyte differentiation by MMP-13 inhibitor small molecule encapsulated in alginate-chondroitin sulfate-platelet lysate hydrogel. *Stem Cell Res Ther* 2020;11(1). <https://doi.org/10.1186/s13287-020-01930-1>.

- [33] Millar VRH, Mangiavini L, Polito U, Canciani B, Nhuyen VT, Cerillo F, et al. Hypoxia as a stimulus for the maturation of meniscal cells: highway to novel tissue engineering strategies? *Int J Mol Sci* 2021;22(13). <https://doi.org/10.3390/ijms22136905>.
- [34] Pattappa G, Johnstone B, Zellner J, Docheva D, Angele P. The importance of physioxia in mesenchymal stem cell chondrogenesis and the mechanisms controlling its response. *Int J Mol Sci* 2019;20(3). <https://doi.org/10.3390/ijms20030484>.
- [35] Taubenberger AV, Woodruff MA, Bai H, Muller DJ, Huttmacher DW. The effect of unlocking RGD-motifs in collagen I on pre-osteoblast adhesion and differentiation. *Biomaterials* 2010;31(10):2827–35. <https://doi.org/10.1016/j.biomaterials.2009.12.051>.
- [36] Heino J. The collagen family members as cell adhesion proteins. *Bioessays* 2007;29(10):1001–10. <https://doi.org/10.1002/bies.20636>.
- [37] IJ J, Yamada KM. *Integrin signa. Ing: -L-; 1997*.
- [38] Salinas CN, Anseth KS. The enhancement of chondrogenic differentiation of human mesenchymal stem cells by enzymatically regulated RGD functionalities. *Biomaterials* 2008;29(15):2370–7. <https://doi.org/10.1016/j.biomaterials.2008.01.035>.
- [39] Bragdon B, Moseychuk O, Saldanha S, King D, Julian J, Nohe A. Bone morphogenetic proteins: a critical review. *Cell Signal* 2011;23(4):609–20. <https://doi.org/10.1016/j.cellsig.2010.10.003>.
- [40] Thielen NGM, van der Kraan PM, van Caam APM. TGF β /BMP signaling pathway in cartilage homeostasis. *Cells* 2019;8(9). <https://doi.org/10.3390/cells8090969>.
- [41] Lim KT, Patel DK, Seonwoo H, Kim J, Chung JH. A fully automated bioreactor system for precise control of stem cell proliferation and differentiation. *Biochem Eng J* 2019;150. <https://doi.org/10.1016/j.bej.2019.107258>.
- [42] van de Walle A, Faissal W, Wilhelm C, Luciani N. Role of growth factors and oxygen to limit hypertrophy and impact of high magnetic nanoparticles dose during stem cell chondrogenesis. *Comput Struct Biotechnol J* 2018;16:532–42. <https://doi.org/10.1016/j.csbj.2018.10.014>.
- [43] Legendre F, Ollitrault D, Gomez-Leduc T, Bouyoucef M, Hervieu M, Gruchy N, et al. Enhanced chondrogenesis of bone marrow-derived stem cells by using a combinatory cell therapy strategy with BMP-2/TGF- β 1, hypoxia, and COL1A1/HtrA1 siRNAs. *Sci Rep* 2017;7(1). <https://doi.org/10.1038/s41598-017-03579-y>.
- [44] Neybecker P, Henrionnet C, Pape E, Mainard D, Galois L, Loeuille D, et al. In vitro and in vivo potentialities for cartilage repair from human advanced knee osteoarthritis synovial fluid-derived mesenchymal stem cells. *Stem Cell Res Ther* 2018;9(1). <https://doi.org/10.1186/s13287-018-1071-2>.
- [45] Cicione C, Muinos-López E, Hermida-Gómez T, Fuentes-Boquete I, Díaz-Prado S, Blanco FJ. Effects of severe hypoxia on bone marrow mesenchymal stem cells differentiation potential. *Stem Cell Int* 2013. <https://doi.org/10.1155/2013/232896>. Published online.